

## Chapter 5

---

---

# Molecular Origin of the Nonlinear Optical Response

In Chapter 3, we presented a general quantum-mechanical theory of the nonlinear optical susceptibility. This calculation was based on time-dependent perturbation theory and led to explicit predictions for the complete frequency dependence of the linear and nonlinear optical susceptibilities. Unfortunately, however, these quantum-mechanical expressions are typically far too complicated to be of use for practical calculations.

In this chapter we review some of the simpler approaches that have been implemented to develop an understanding of the nonlinear optical characteristics of various materials. Many of these approaches are based on understanding the optical properties at the molecular level. We also present brief descriptions of the nonlinear optical characteristics of conjugated polymers, chiral molecules, and liquid crystals.

### 5.1 Nonlinear Susceptibilities Calculated Using Time-Independent Perturbation Theory

One approach to the practical calculation of nonlinear optical susceptibilities is based on the use of time-independent perturbation theory (see, e.g., Jha and Bloembergen, 1968 or Ducuing, 1977). The motivation for using this approach is that time-independent perturbation theory is usually much easier to implement than time-dependent perturbation theory. The justification of the use of this approach is that one is often interested in the study of nonlinear optical interactions in the highly nonresonant limit  $\omega \ll \omega_0$  (where  $\omega$  is the optical frequency and  $\omega_0$  is the resonance frequency of the material system), in order to avoid absorption losses. For  $\omega \ll \omega_0$ , the optical field can to good approximation be taken to be a quasi-static quantity.

To see how this method proceeds, let us represent the polarization of a material system in the usual form\*

$$\tilde{P} = \epsilon_0 \chi^{(1)} \tilde{E} + \epsilon_0 \chi^{(2)} \tilde{E}^2 + \epsilon_0 \chi^{(3)} \tilde{E}^3 + \dots \quad (5.1.1)$$

We can then calculate the energy stored in polarizing the medium as

$$\begin{aligned} W &= - \int_0^{\tilde{E}} \tilde{P}(\tilde{E}') d\tilde{E}' = -\frac{1}{2} \chi^{(1)} \tilde{E}^2 - \frac{1}{3} \chi^{(2)} \tilde{E}^3 - \frac{1}{4} \chi^{(3)} \tilde{E}^4 \dots \\ &\equiv W^{(2)} + W^{(3)} + W^{(4)} + \dots \end{aligned} \quad (5.1.2)$$

The significance of this result is that it shows that if we know  $W$  as a function of  $\tilde{E}$  (either by calculation or, for instance, from Stark effect measurements), we can use this knowledge to deduce the various orders of susceptibility  $\chi^{(n)}$ . For instance, if we know  $W$  as a power series in  $\tilde{E}$  we can determine the susceptibilities as†

$$\chi^{(n-1)} = -\frac{n W^{(n)}}{\epsilon_0 \tilde{E}^n}. \quad (5.1.3)$$

More generally, even if the power series expansion is not known, the nonlinear susceptibilities can be obtained through differentiation as

$$\chi^{(n-1)} = \frac{-1}{\epsilon_0 (n-1)!} \left. \frac{\partial^n W}{\partial \tilde{E}^n} \right|_{E=0}. \quad (5.1.4)$$

Before turning our attention to the general quantum-mechanical calculation of  $W^{(n)}$ , let us see how to apply the result given by Eq. (5.1.3) to the special case of the hydrogen atom.

### 5.1.1 Hydrogen Atom

From considerations of the Stark effect, it is well known how to calculate the ground-state energy  $w$  of the hydrogen atom as a function of the strength  $E$  of an applied electric field (Schiff, 1968; Sewell, 1949). We shall not present the details of the calculation here, both because they are readily available in the scientific literature and because the simplest method

\* As a notational convention, in the present discussion we retain the tilde over  $P$  and  $E$  both for slowly varying (quasi-static) and for fully static fields.

† For time-varying fields, Eq. (5.1.3) still holds, but with  $W^{(n)}$  and  $\tilde{E}^n$  replaced by their time averages, that is, by  $\langle W^{(n)} \rangle$  and  $\langle \tilde{E}^n \rangle$ . For  $\tilde{E} = E e^{-i\omega t} + \text{c.c.}$ , one finds that  $\tilde{E} = 2E \cos(\omega t + \phi)$ , and  $\tilde{E}^n = 2^n E^n \cos^n(\omega t + \phi)$ , so that  $\langle \tilde{E}^n \rangle = 2^n E^n \langle \cos^n(\omega t + \phi) \rangle$ . Note that  $\langle \cos^2(\omega t + \phi) \rangle = 1/2$  and  $\langle \cos^4(\omega t + \phi) \rangle = 3/8$ .

for obtaining this result makes use of the special symmetry properties of the hydrogen atom and does not readily generalize to other situations. One finds that

$$\frac{w}{2R} = -\frac{1}{2} - \frac{9}{4} \left( \frac{E}{E_{\text{at}}} \right)^2 - \frac{3555}{64} \left( \frac{E}{E_{\text{at}}} \right)^4 + \dots, \quad (5.1.5)$$

where  $R = me^4/32\pi^2\epsilon_0^2\hbar^2 = 13.6$  eV is the Rydberg constant and where  $E_{\text{at}} = e/4\pi\epsilon_0 a_0^2 = m^2 e^5/(4\pi\epsilon_0)^3 \hbar^4 = 5.14 \times 10^{11}$  V/m is the atomic unit of electric field strength. We now take  $W$  to be given by  $W = Nw$ , where  $N$  is the number density of atoms, and introduce Eq. (5.1.5) into Eq. (5.1.3). We thus find that

$$\chi^{(1)} = N\alpha \quad \text{where} \quad \alpha = \frac{9}{2} a_0^3, \quad (5.1.6a)$$

$$\chi^{(3)} = N\gamma \quad \text{where} \quad \gamma = \frac{3555}{16} \frac{a_0^7}{e^6}, \quad (5.1.6b)$$

where  $a_0 = 4\pi\epsilon_0\hbar^2/me^2$  is the Bohr radius. Note that these results conform with standard scaling laws for nonresonant polarizabilities

$$\alpha \simeq \text{atomic volume } V, \quad (5.1.7a)$$

$$\gamma \propto V^{7/3}. \quad (5.1.7b)$$

### 5.1.2 General Expression for the Nonlinear Susceptibility in the Quasi-Static Limit

A standard problem in quantum mechanics involves determining how the energy of some state  $|\psi_n\rangle$  of an atomic system is modified in response to a perturbation of the atom. To treat this problem mathematically, we assume that the Hamiltonian of the system can be represented as

$$\hat{H} = \hat{H}_0 + \hat{V}, \quad (5.1.8)$$

where  $\hat{H}_0$  represents the total energy of the free atom and  $\hat{V}$  represents the quasi-static perturbation due to some external field. For the problem at hand we assume that

$$\hat{V} = -\hat{\mu}\tilde{E}, \quad (5.1.9)$$

where  $\hat{\mu} = -e\hat{x}$  is the electric dipole moment operator and  $\tilde{E}$  is an applied quasi-static field. We require that the atomic wavefunction obey the time-independent Schrödinger equation

$$\hat{H}|\psi_n\rangle = w_n|\psi_n\rangle. \quad (5.1.10)$$

For most situations of interest, Eqs. (5.1.8)–(5.1.10) cannot be solved in closed form, and must be solved using perturbation theory. One represents the energy  $w_n$  and state vector  $|\psi_n\rangle$  as power series in the perturbation as

$$w_n = w_n^{(0)} + w_n^{(1)} + w_n^{(2)} + \dots, \quad (5.1.11a)$$

$$|\psi_n\rangle = |\psi_n^{(0)}\rangle + |\psi_n^{(1)}\rangle + |\psi_n^{(2)}\rangle + \dots. \quad (5.1.11b)$$

The details of the procedure are well documented in the scientific literature; see, for instance, Dalgarno (1961). One finds that the energies are given by

$$w_n^{(1)} = e\tilde{E}\langle n|x|n\rangle, \quad (5.1.12a)$$

$$w_n^{(2)} = e^2\tilde{E}^2\sum'_s \frac{\langle n|x|s\rangle\langle s|x|n\rangle}{w_s^{(0)} - w_n^{(0)}}, \quad (5.1.12b)$$

$$w_n^{(3)} = e^3\tilde{E}^3\sum'_{st} \frac{\langle n|x|s\rangle\langle s|x|t\rangle\langle t|x|n\rangle}{(w_s^{(0)} - w_n^{(0)})(w_t^{(0)} - w_n^{(0)})}, \quad (5.1.12c)$$

$$w_n^{(4)} = e^4\tilde{E}^4\sum'_{stu} \frac{\langle n|x|s\rangle\langle s|x|t\rangle\langle t|x|u\rangle\langle u|x|n\rangle}{(w_s^{(0)} - w_n^{(0)})(w_t^{(0)} - w_n^{(0)})(w_u^{(0)} - w_n^{(0)})} \\ - e^2\tilde{E}^2w_n^{(2)}\sum'_u \frac{\langle n|x|u\rangle\langle u|x|n\rangle}{(w_u^{(0)} - w_n^{(0)})^2}. \quad (5.1.12d)$$

The prime following each summation symbol indicates that the state  $n$  is to be omitted from the indicated summation. Through use of these expressions one can deduce explicit forms for the linear and nonlinear susceptibilities. We let  $W = Nw$ , assume that the state of interest is the ground state  $g$ , and make use of Eqs. (5.1.3) to find that

$$\chi^{(1)} = N\alpha, \quad \alpha = \alpha_{xx} = \frac{2e^2}{\hbar} \sum_{s \neq g} \frac{x_{gs}x_{sg}}{\omega_{sg}}, \quad (5.1.13a)$$

$$\chi^{(2)} = N\beta, \quad \beta = \beta_{xxx} = \frac{3e^3}{\hbar^2} \sum_{s,t \neq g} \frac{x_{gt}x_{ts}x_{sg}}{\omega_{tg}\omega_{sg}}, \quad (5.1.13b)$$

$$\chi^{(3)} = N\gamma, \quad \gamma = \gamma_{xxx} = \frac{4e^4}{\hbar^3} \left( \sum_{s,t,u \neq g} \frac{x_{gu}x_{ut}x_{ts}x_{sg}}{\omega_{ug}\omega_{tg}\omega_{sg}} - \sum_{s,t \neq g} \frac{x_{gt}x_{tg}x_{gs}x_{sg}}{\omega_{tg}\omega_{sg}^2} \right), \quad (5.1.13c)$$

where  $\hbar\omega_{sg} = w_s^{(0)} - w_g^{(0)}$ , and so on. We see that  $\chi^{(3)}$  naturally decomposes into the sum of two terms, which can be represented schematically in terms of the two diagrams shown in Fig. 5.1.1. Note that this result is entirely consistent with the predictions of the model of the

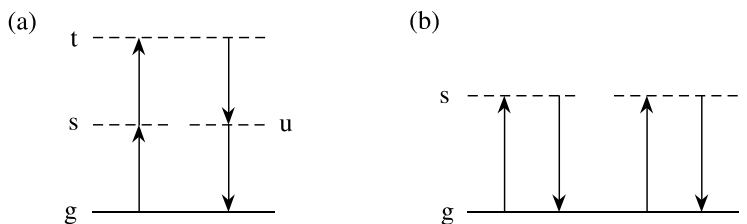


FIGURE 5.1.1: Schematic representation of the two terms appearing in Eq. (5.1.13c).

nonlinear susceptibility based on time-dependent perturbation theory (see Eq. (4.3.12)), but is more simply obtained by the present formalism.

Eqs. (5.1.13) constitute the quantum-mechanical predictions for the static values of the linear and nonlinear susceptibilities. Evaluation of these expressions can be still quite demanding, as it requires knowledge of all of the resonance frequencies and dipole transition moments connecting to the atomic ground state. Several approximations can be made to simplify these expressions. One example is the Unsöld approximation, which entails replacing each resonance frequency (e.g.,  $\omega_{sg}$ ) by some average transition frequency  $\omega_0$ . The expression (5.1.13a) for the linear polarizability then becomes

$$\alpha = \frac{2e^2}{\hbar\omega_0} \sum_s' \langle g|x|s \rangle \langle s|x|g \rangle. \quad (5.1.14)$$

We formally rewrite this expression as

$$\alpha = \frac{2e^2}{\hbar\omega_0} \langle g|x\hat{O}x|g \rangle \quad \text{where} \quad \hat{O} = \sum_s' |s \rangle \langle s|. \quad (5.1.15)$$

We now replace  $\hat{O}$  by the unrestricted sum

$$\hat{O} = \sum_s |s \rangle \langle s|, \quad (5.1.16)$$

which we justify by noting that for states of fixed parity  $\langle g|x|g \rangle$  vanishes, and thus it is immaterial whether or not the state  $g$  is included in the sum over all  $s$ . We next note that

$$\sum_s |s \rangle \langle s| = 1 \quad (5.1.17)$$

by the closure assumption of quantum mechanics. We thus find that

$$\alpha = \frac{2e^2}{\hbar\omega_0} \langle x^2 \rangle. \quad (5.1.18a)$$

This result shows that the linear susceptibility is proportional to the electric quadrupole moment of the ground-state electron distribution. We can apply similar reasoning to the simplification

of the expressions for the second- and third-order nonlinear coefficients to find that

$$\beta = -\frac{3e^3}{\hbar^2\omega_0^2}\langle x^3 \rangle, \quad (5.1.18b)$$

$$\gamma = \frac{4e^4}{\hbar^3\omega_0^3}[\langle x^4 \rangle - 2\langle x^2 \rangle^2]. \quad (5.1.18c)$$

These results show that the hyperpolarizabilities can be interpreted as measures of various higher-order moments of the ground state electron distribution. Note that the linear polarizability and hyperpolarizabilities increase rapidly with the physical dimensions of the electron cloud associated with the atomic ground state. Note further that Eqs. (5.1.18a) and (5.1.18c) can be combined to express  $\gamma$  in the intriguing form

$$\gamma = \alpha^2 \frac{g}{\hbar\omega_0} \quad \text{where} \quad g = \left[ \frac{\langle x^4 \rangle}{\langle x^2 \rangle^2} - 2 \right]. \quad (5.1.19)$$

Here  $g$  is a dimensionless quantity (known in statistics as the kurtosis) that provides a measure of the normalized fourth moment of the ground-state electron distribution.

These expressions can be simplified still further by noting that within the context of the present model the average transition frequency  $\omega_0$  can itself be represented in terms of the moments of  $x$ . We start with the Thomas–Reiche–Kuhn sum rule (see, for instance, Eq. (61) of Bethe and Salpeter, 1977), which states that

$$\frac{2m}{\hbar} \sum_k \omega_{kg} |x_{kg}|^2 = Z, \quad (5.1.20)$$

where  $Z$  is the number of optically active electrons. If we now replace  $\omega_{kg}$  by the average transition frequency  $\omega_0$  and perform the summation over  $k$  in the same manner as in the derivation of Eq. (5.1.18a), we obtain

$$\omega_0 = \frac{Z\hbar}{2m\langle x^2 \rangle}. \quad (5.1.21)$$

This expression for  $\omega_0$  can now be introduced into Eqs. (5.1.18) to obtain

$$\alpha = \frac{4e^2m}{Z\hbar^2}\langle x^2 \rangle^2, \quad (5.1.22)$$

$$\beta = -\frac{12e^3m^2}{Z^2\hbar^4}\langle x^2 \rangle^2\langle x^3 \rangle, \quad (5.1.23)$$

$$\gamma = \frac{32e^4m^3}{Z^3\hbar^6}\langle x^2 \rangle^3(\langle x^4 \rangle - 2\langle x^2 \rangle^2). \quad (5.1.24)$$

Note that these formulas can be used to infer scaling laws relating the optical constants to the characteristic size  $L$  of a molecule. In particular, one finds that  $\alpha \sim L^4$ ,  $\beta \sim L^7$ , and  $\gamma \sim L^{10}$ . Note the important result that nonlinear coefficients increase rapidly with the size of a molecule. Note also that  $\alpha$  is a measure of the electric quadrupole moment of the ground-state electron distribution,  $\beta$  is a measure of the octopole moment of the ground-state electron distribution, and  $\gamma$  depends on both the hexadecapole and the quadrupole moment of the electron ground-state electron distribution.\*

## 5.2 Semiempirical Models of the Nonlinear Optical Susceptibility

We noted earlier in Section 1.4 that Miller's rule can be successfully used to predict the second-order nonlinear optical properties of a broad range of materials. Miller's rule can be generalized to third-order nonlinear optical interactions, where it takes the form

$$\chi^{(3)}(\omega_4, \omega_3, \omega_2, \omega_1) = A \chi^{(1)}(\omega_4) \chi^{(1)}(\omega_3) \chi^{(1)}(\omega_2) \chi^{(1)}(\omega_1), \quad (5.2.1)$$

where  $\omega_4 = \omega_1 + \omega_2 + \omega_3$  and where  $A$  is a quantity that is assumed to be frequency independent and nearly the same for all materials. Wynne (1969) has shown that this generalization of Miller's rule is valid for certain optical materials, such as ionic crystals. However, this generalization is not universally valid.

Wang (1970) has proposed a different relation that seems to be more generally valid. Wang's relation is formulated for the nonlinear optical response in the quasi-static limit and states that

$$\chi^{(3)} = Q' (\chi^{(1)})^2, \quad \text{where} \quad Q' = g' / N_{\text{eff}} \hbar \omega_0, \quad (5.2.2)$$

and where  $N_{\text{eff}} = Nf$  is the product of the molecular number density  $N$  with the oscillator strength  $f$ ,  $\omega_0$  is an average transition frequency, and  $g'$  is a dimensionless parameter of the order of unity that is assumed to be nearly the same for all materials. Wang has shown empirically that the predictions of Eq. (5.2.2) are accurate both for low-pressure gases (where Miller's rule does not make accurate predictions) and for ionic crystals (where Miller's rule does make accurate predictions). By comparison of this relation with Eq. (5.1.19), we see that  $g'$  is intimately related to the kurtosis of the ground-state electron distribution. There does not seem to be any simple physical argument for why the quantity  $g'$  should be the same for all materials.

---

\* There is an additional contribution to the hyperpolarizability  $\beta$  resulting from the difference in permanent dipole moment between the ground and excited states. This contribution is not accounted for by the present model.

## Model of Boling, Glass, and Owyong

The formula (Eq. 5.2.2) of Wang serves as a starting point for the model of Boling et al. (1978), which allows one to predict the nonlinear refractive index constant  $n_2$  on the basis of linear optical properties. One assumes that the linear refractive index is described by the Lorentz–Lorenz law (see Eq. (3.9.8a)) and Lorentz oscillator model (see Eq. (1.4.17) or Eq. (3.5.25)) as

$$\frac{n^2 - 1}{n^2 + 2} = \frac{1}{3} N \alpha, \quad (5.2.3a)$$

$$\alpha = \frac{f e^2 / m}{\omega_0^2 - \omega^2}, \quad (5.2.3b)$$

where  $f$  is the oscillator strength of the transition making the dominant contribution to the optical properties. Note that by measuring the refractive index as a function of frequency it is possible through use of these equations to determine both the resonance frequency  $\omega_0$  and the effective number density  $Nf$ . The nonlinear refractive index is determined from the standard set of equations

$$n_2 = \frac{3}{4n^2\epsilon_0 c} \chi^{(3)}, \quad \chi^{(3)} = L^4 N \gamma, \quad L = \frac{n^2 + 2}{3}, \quad (5.2.4a)$$

$$\gamma = \frac{g \alpha^2}{\hbar \omega_0}. \quad (5.2.4b)$$

Eq. (5.2.4b) is the microscopic form of Wang's formula (5.2.2), where  $g$  is considered to be a free parameter. If Eq. (5.2.3b) is solved for  $\alpha$ , which is then introduced into Eq. (5.2.4b), and use is made of Eqs. (5.2.4a), we find that the expression for  $n_2$  is given by

$$n_2 = \frac{(n^2 + 2)^2 (n^2 - 1)^2 (gf)}{6n^2 \epsilon_0 c \hbar \omega_0 (Nf)}. \quad (5.2.5)$$

This equation gives a prediction for  $n_2$  in terms of the linear refractive index  $n$ , the quantities  $\omega_0$  and  $(Nf)$  which (as described above) can be deduced from the dispersion in the refractive index, and the combination  $(gf)$ , which is considered to be a constant quantity for a broad range of optical materials. The value  $(gf) = 3$  is found empirically to give good agreement with measured values. A comparison of the predictions of this model with measured values of  $n_2$  has been performed by Adair et al. (1989), and some of their results are shown in Fig. 5.2.1. The two theoretical curves shown in this figure correspond to two different choices of the parameter  $(gf)$  of Eq. (5.2.5). Lenz et al. (2000) have described a model related to that of Boling et al. that has good predictive value for describing the nonlinear optical properties of chalcogenide glasses.



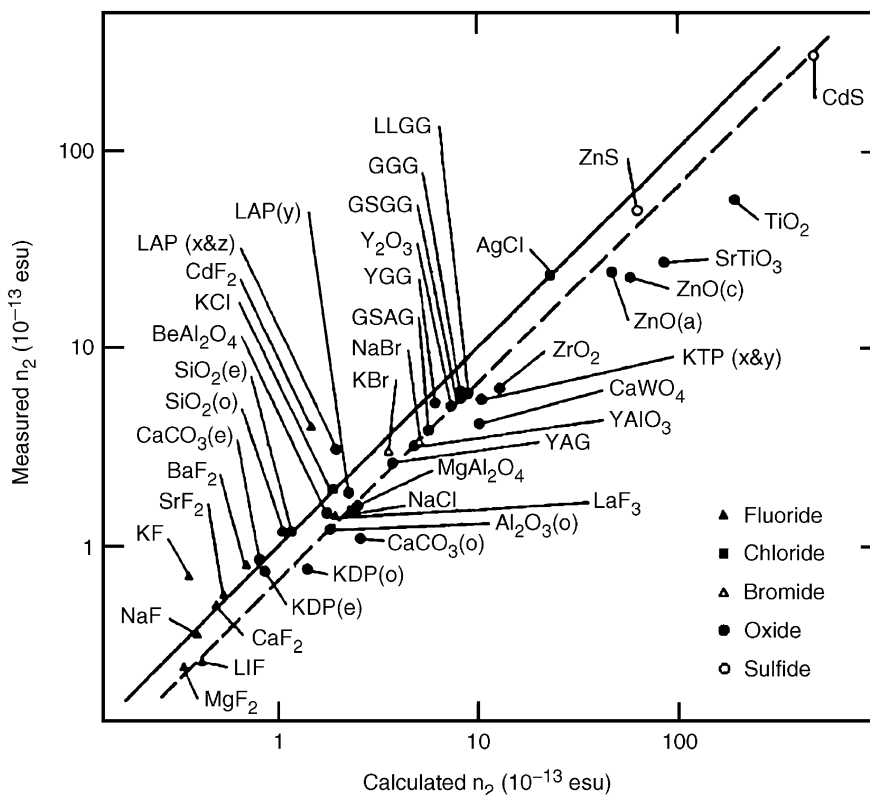


FIGURE 5.2.1: Comparison of the predictions of Eq. (5.2.5) with experimental results. After Adair et al. (1989).

### 5.3 Nonlinear Optical Properties of Conjugated Polymers

Certain polymers known as conjugated polymers can possess an extremely large nonlinear optical response. For example, a certain form of polydiacetylene known as PTS possesses a third-order susceptibility of  $3.5 \times 10^{-18} \text{ m}^2/\text{V}^2$ , as compared to the value of  $2.7 \times 10^{-20} \text{ m}^2/\text{V}^2$  for carbon disulfide. In this section some of the properties of conjugated polymers are described.

A polymer is said to be conjugated if it contains alternating single and double (or single and triple) bonds. Alternatively, a polymer is said to be saturated if it contains only single bonds. A special class of conjugated polymers is the polyenes, which are molecules that contain many double bonds.

Part (a) of Fig. 5.3.1 shows the structure of polyacetylene, a typical chainlike conjugated polymer. According to convention, the single lines in this diagram represent single bonds and double lines represent double bonds. A single bond always has the structure of a  $\sigma$  bond, which is shown schematically in part (b) of the figure. In contrast, a double bond consists of a  $\sigma$  bond

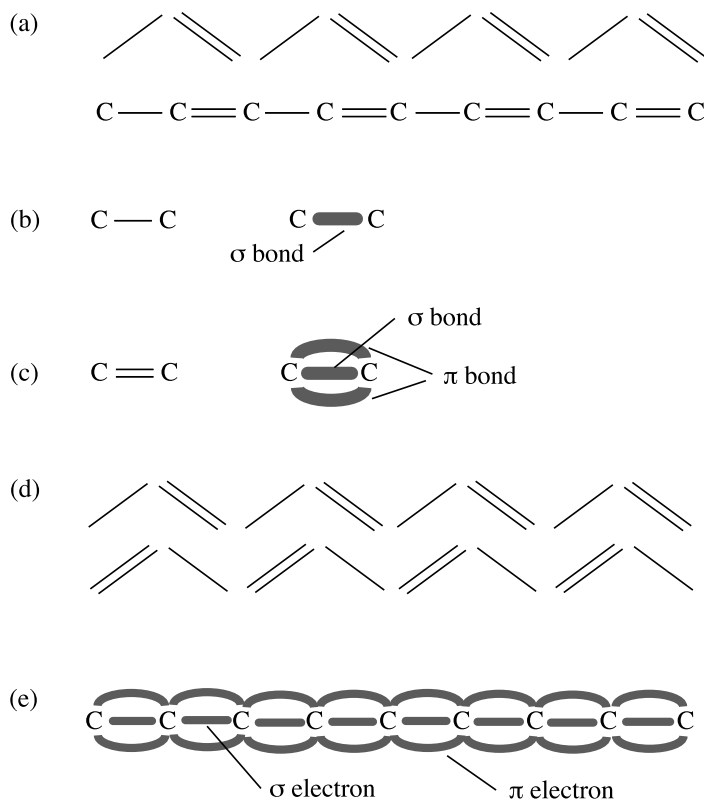


FIGURE 5.3.1: (a) Two common representations of a conjugated chainlike polymer. (b) Standard representation of a single bond (left) and a schematic representation of the electron charge distribution of the single bond (right). (c) Standard representation of a double bond (left) and a schematic representation of the electron charge distribution of the double bond (right). (d) Two representations of the same polymer chain with the locations of the single and double bonds interchanged, suggesting the arbitrariness of which bond is called the single bond and which is called the double bond in an actual polymer chain. (e) Representation of the charge distribution of a conjugated chainlike polymer.

and a  $\pi$  bond, as shown in part (c) of the figure. A  $\pi$  bond is made up of the overlap of two  $p$  orbitals, one from each atom that is connected by the bond.

The optical response of  $\sigma$  bonds is very different from that of  $\pi$  bonds because  $\sigma$  electrons (that is, electrons contained in a  $\sigma$  bond) tend to be localized in space. In contrast,  $\pi$  electrons tend to be delocalized. Because  $\pi$  electrons are delocalized, they tend to be less tightly bound and can respond more freely to an applied optical field. They thus tend to produce larger linear and nonlinear optical responses.

$\pi$  electrons tend to be delocalized in the sense that a given electron can be found anywhere along the polymer chain. They are delocalized because (unlike the  $\sigma$  electrons) they tend to be

located at some distance from the symmetry axis. In addition, even though one conventionally draws a polymer chain in the form shown in part (a) of the figure, for a long chain it would be equally valid to exchange the locations of the single and double bonds. The actual form of the polymer chain is thus a superposition of the two configurations shown in part (d) of the figure. This perspective is reinforced by noting that  $p$  orbitals extend both to the left and to the right of each carbon atom, and thus there is considerable arbitrariness as to which bonds we should call single bonds and which we should call double bonds. Thus, the actual electron distribution might look more like that shown in part (e) of the figure.

As an abstraction, one can model the  $\pi$  electrons of a conjugated chainlike polymer as being entirely free to move in a one-dimensional square-well potential whose length  $L$  is that of the polymer chain. Rustagi and Ducuing (1974) performed such a calculation and found that the linear and third-order polarizabilities are given by

$$\alpha = \frac{8L^3}{3a_0\pi^2\mathcal{N}} \quad \text{and} \quad \gamma = \frac{256L^5}{45a_0^3e^2\pi^6\mathcal{N}^5}, \quad (5.3.1)$$

where  $\mathcal{N}$  is the number of electrons per unit length and  $a_0$  is the Bohr radius. (See also Problem 3 at the end of this chapter.) It should be noted that the linear optical response increases rapidly with the length  $L$  of the polymer chain and that the nonlinear optical response increases even more rapidly. Of course, for condensed matter, the number of polymer chains per unit volume  $N$  will decrease with increasing chain length  $L$ , so the susceptibilities  $\chi^{(1)}$  and  $\chi^{(3)}$  will increase less rapidly with  $L$  than do  $\alpha$  and  $\beta$  themselves. Nonetheless, the present model predicts that conjugated polymers in the form of long chains should possess extremely large values of the nonlinear optical susceptibility. Some experimental results that confirm the  $L^5$  dependence of the hyperpolarizability are shown in Fig. 5.3.2. Large values of the nonlinear optical response has also been studied for the material  $C_{60}$ , which consists of essentially free electrons constrained to lie on the surface of a sphere (Blau et al., 1991).

## 5.4 Bond-Charge Model of Nonlinear Optical Properties

In a collection of free atoms, the natural basis for describing the optical properties of the atomic system is the set of energy eigenstates of the individual atoms. However, when atoms are arranged in a crystal lattice, it becomes more natural to think of the outer electrons as being localized within the bonds that confine the atoms to their lattice sites. (The inner-core electrons are so tightly bound that they make negligible contribution to the optical response in any case.) Extensive evidence shows that one can ascribe a linear polarizability and higher-order polarizabilities to each bond in a molecule or crystalline solid (Levine, 1969; Chemla, 1971). This evidence also shows that the polarizability of one bond is reasonably unaffected by the nature of nearby bonds. Thus, the susceptibility of a complex system can be

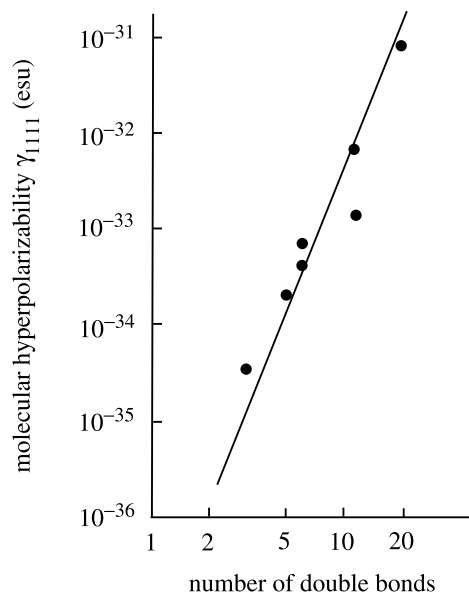


FIGURE 5.3.2: Measured dependence of the value of the hyperpolarizability  $\gamma_{1111}$  on the number of double bonds in the molecule. The data are from Hermann and Ducuing (1974) and the straight line has a slope of 5 in accordance with Eq. (5.3.1). To convert  $\gamma$  to SI units of  $\text{m}^5/\text{V}^2$ , multiply each value by  $1.4 \times 10^{-14}$ .

predicted by summing (taking proper account of their orientation) the responses of the various bonds present in the material. Bond hyperpolarizabilities can be determined either experimentally or by one of several different theoretical approaches.

The bond-charge model is illustrated in Fig. 5.4.1. Part (a) of this figure shows a bond connecting atoms  $A$  and  $B$ . As an idealization, the bond is considered to be a point charge of charge  $q$  located between the two ions. The quantities  $r_A$  and  $r_B$  are the covalent radii of atoms  $A$  and  $B$  and  $d = r_A + r_B$  is known as the bond length. According to Levine (1973), the bond charge is given by

$$q = en_v(1/\epsilon + \frac{1}{3}f_c), \quad (5.4.1)$$

where  $n_v$  is the number of electrons per bond,  $\epsilon$  is the static dielectric constant of the material, and  $f_c$  is a parameter known as the fractional degree of covalency of the bond.

Part (b) of Fig. 5.4.1 shows how the bond charge  $q$  moves in the presence of an electric field  $\mathbf{E}$  that is oriented parallel to the bond axis. The charge is seen to move by an amount  $\delta r = \alpha_{\parallel} E/q$ , where  $\alpha_{\parallel}$  is the polarizability measured along the bond axis, and consequently the ion-to-bond-charge distances  $r_A$  and  $r_B$  change by amounts

$$-\Delta r_A = \Delta r_B = \delta r = \alpha_{\parallel} E/q. \quad (5.4.2)$$

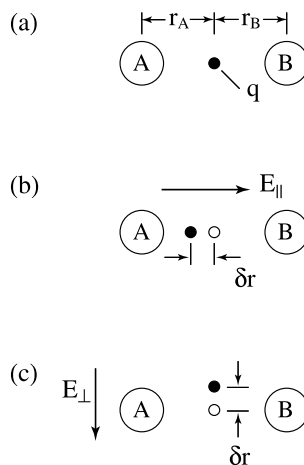


FIGURE 5.4.1: The bond-charge model applied to a chemical bond between constituents  $A$  and  $B$ . Parts (b) and (c) show how the charge moves in response to applied electric fields.

Part (c) of the figure shows how the bond charge moves when  $\mathbf{E}$  is applied perpendicular to the bond axis. In this case  $\delta r = \alpha_{\perp} E/q$ , and to lowest order the distances  $r_A$  and  $r_B$  change by amounts

$$\Delta r_A = \frac{\delta r^2}{2r_A} = \frac{\alpha_{\perp}^2 E^2}{2r_A q^2}, \quad (5.4.3a)$$

$$\Delta r_B = \frac{\delta r^2}{2r_B} = \frac{\alpha_{\perp}^2 E^2}{2r_B q^2}. \quad (5.4.3b)$$

We see that a field parallel to the bond axis can induce a linear change in the distances  $r_A$  and  $r_B$ , but that a field perpendicular to the axis can induce only a second-order change in these quantities.

Let us now see how to make quantitative predictions using the bond-charge model (Chemla et al., 1974). According to Phillips (1967) and Van Vechten (1969), the (linear) bond polarizability can be represented as

$$\alpha \equiv \frac{1}{3}(\alpha_{\parallel} + 2\alpha_{\perp}) = (2a_0)^3 D \frac{E_0^2}{E_g^2}, \quad (5.4.4)$$

where  $a_0 = 4\pi\epsilon_0\hbar^2/me^2$  is the Bohr radius,  $E_0 = me^4/2(4\pi\epsilon_0)^2\hbar^2$  is the Rydberg unit of energy,  $D$  is a numerical factor of the order of unity, and  $E_g$  is the mean energy gap associated with the bond. This quantity can be represented as

$$E_g^2 = E_h^2 + C^2, \quad (5.4.5)$$

where  $E_h$  is the homopolar contribution given by

$$E_h = 40d^{-2.5}, \quad (5.4.6a)$$

and where  $C$  is the heteropolar contribution given by

$$C = 1.5e^{-kR} \left( \frac{z_A}{r_A} - \frac{z_B}{r_B} \right) e^2, \quad (5.4.6b)$$

where  $z_A$  and  $z_B$  are the number of valence electrons on atoms  $A$  and  $B$ , respectively, and where  $\exp(-kR)$  is the Thomas–Fermi screening factor, with  $R = \frac{1}{2}(r_A + r_B) = \frac{1}{2}d$ . The numerical factor in Eq. (5.4.6a) presupposes that  $d$  is measured in angstroms and  $E_h$  in electron volts.

The bond-charge model ascribes the nonlinear optical response of a material system to the variation of the bond polarizability  $\alpha_{ij}$  induced by an applied field  $E_j$ . Explicitly one expresses the bond dipole moment as

$$\begin{aligned} p_i &= p_i^{(1)} + p_i^{(2)} + p_i^{(3)} + \cdots \\ &= \left[ (\alpha_{il})_0 + \left( \frac{\partial \alpha_{il}}{\partial E_j} \right) E_j + \frac{1}{2} \left( \frac{\partial^2 \alpha_{il}}{\partial E_j \partial E_k} \right) E_j E_k \right] E_l + \cdots \\ &\equiv (\alpha_{il})_0 E_l + \beta_{ijk} E_j E_l + \gamma_{ijkl} E_j E_k E_l + \cdots \end{aligned} \quad (5.4.7)$$

Let us now calculate the hyperpolarizabilities  $\beta_{ijk}$  and  $\gamma_{ijkl}$ . Since the model assumes that the bonds are axially symmetric, the only nonvanishing components of the hyperpolarizabilities are

$$\beta_{\parallel} = \beta_{zzz}, \quad \beta_{\perp} = \beta_{xxz}, \quad (5.4.8a)$$

$$\gamma_{\parallel} = \gamma_{zzzz}, \quad \gamma_{\perp} = \gamma_{xxxx}, \quad \gamma_{\parallel\perp} = \gamma_{zzxx}, \quad (5.4.8b)$$

where we have assumed that  $z$  lies along the bond axis. We next note that, as a consequence of Eqs. (5.4.3), a transverse field  $E_{\perp}$  cannot produce a first-order (or in fact any odd-order) change in  $\alpha_{ij}$ , that is,

$$\left( \frac{\partial}{\partial E_{\perp}} \right)^q \alpha_{ij} = 0 \quad \text{for } q \text{ odd.} \quad (5.4.9)$$

We also note that the present model obeys Kleinman symmetry, since it does not consider the frequency dependence of any of the optical properties. Because of Kleinman symmetry, we can express  $\beta_{\perp} \equiv \partial \alpha_{xx} / \partial E_z$  as

$$\beta_{\perp} = \frac{\partial \alpha_{xz}}{\partial E_x}, \quad (5.4.10)$$

which vanishes by Eq. (5.4.9). We likewise find that

$$\gamma_{\parallel\perp} = \frac{1}{2} \frac{\partial^2 \alpha_{xz}}{\partial E_x \partial E_z} = 0. \quad (5.4.11)$$

We thus deduce that the only nonvanishing components are  $\beta_{\parallel}$ ,  $\gamma_{\parallel}$ , and  $\gamma_{\perp}$ , which can be expressed as

$$\beta_{\parallel} = \frac{\partial \alpha_{\parallel}}{\partial E_{\parallel}} = 3 \frac{\partial \alpha}{\partial E_{\parallel}}, \quad (5.4.12a)$$

$$\gamma_{\parallel} = \frac{\partial^2 \alpha_{\parallel}}{\partial E_{\parallel}^2} = \frac{3}{2} \frac{\partial^2 \alpha}{\partial E_{\parallel}^2}, \quad (5.4.12b)$$

$$\gamma_{\perp} = \frac{\partial^2 \alpha_{\perp}}{\partial E_{\perp}^2} = \frac{3}{4} \frac{\partial^2 \alpha}{\partial E_{\perp}^2}. \quad (5.4.12c)$$

The equations just presented provide the basis of the bond-charge model. The application of this model requires extensive numerical computation which will not be reproduced here. In brief summary, the quantities  $E_h$  and  $C$  of Eqs. (5.4.6) are developed in power series in the applied fields  $E_{\parallel}$  and  $E_{\perp}$  through use of Eqs. (5.4.2) and (5.4.3). Expression (5.4.4) for  $\alpha$  can then be expressed in a power series in the applied field, and the hyperpolarizabilities can be extracted from this power series expression through use of Eqs. (5.4.12). Finally, susceptibilities  $\chi_{ijk}^{(2)}$  and  $\chi_{ijkl}^{(3)}$  are determined by summing over all bonds in a unit volume, taking account of the orientation of each particular bond. This model has been shown to provide good predictive value. For instance, Chemla et al. (1974) have found that this model provides  $\sim 30\%$  accuracy in calculating the third-order nonlinear optical response for Ge, Si, and GaAs. Table 5.4.1 gives values of some measured bond hyperpolarizabilities. In addition Levine (1973) provides extensive tables comparing the predictions of this model with experimental results.

TABLE 5.4.1: Representative bond hyperpolarizabilities  $\gamma$  in units of  $1.4 \times 10^{-50} \text{ m}^5/\text{V}^2$ .<sup>a</sup>

Bond	$\lambda = 1.064 \text{ } \mu\text{m}$	$\lambda = 1.907 \text{ } \mu\text{m}$
C–Cl	$0.90 \pm 0.04$	0.7725
C–H	$0.05 \pm 0.04$	–0.0275
O–H	$0.42 \pm 0.02$	0.5531
C–C	$0.32 \pm 0.42$	0.6211
C=C	$1.03 \pm 1.52$	0.61
C–O	$0.24 \pm 0.19$	0.30
C=O	$0.82 \pm 1.1$	0.99

<sup>a</sup> After Kajzar and Messier (1985).

## 5.5 Nonlinear Optics of Chiral Media

Special considerations apply to the analysis of the nonlinear optical properties of a medium composed of a collection of chiral molecules. A chiral molecule is a molecule with a “handedness,” that is, the mirror image of such a molecule looks different from the molecule itself. By way of example, simple molecules such as  $\text{CS}_2$ ,  $\text{H}_2\text{O}$ ,  $\text{CH}_4$  are achiral (that is, are not chiral) and are identical to their mirror images; however, many organic molecules including simple sugars such as dextrose are chiral.

In the context of linear optics, it is well known that chiral media display the property of optical activity, that is, the rotation of the direction of linear polarization of a light beam as it passes through such a material. (See, for instance, Jenkins and White, 1976.) A material is said to be dextrorotatory if the direction of the polarization rotates in a clockwise sense (looking into the beam) as the beam propagates; if the polarization rotates counterclockwise, the medium is said to be levorotatory. Two molecules that are mirror images of each other are said to be enantiomers. An equal mixture of two enantiomers is said to be a racemic mixture. Optical activity obviously vanishes for a racemic mixture.

Let us now turn to a discussion of the nonlinear optical properties of chiral materials. A liquid composed of chiral molecules is isotropic but nonetheless noncentrosymmetric (see Fig. 5.5.1), and thus it can possess a second-order nonlinear optical response. As we shall see, such a medium can produce sum- or difference-frequency generation, but not second-harmonic generation, and moreover can produce sum- or difference-frequency generation only if the two input beams are non-collinear. The theory of second-order processes in chiral media was developed by Giordmaine (1965) and was studied experimentally by Rentzipis et al. (1966). More recent research on the nonlinear optics of chiral media includes that of Verbiest et al. (1998).

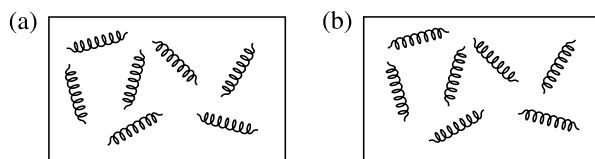


FIGURE 5.5.1: (a) A collection of right-handed spirals and (b) a collection of left-handed spirals. Each medium is isotropic (looks the same in all directions), but neither possesses a center of inversion symmetry.

Let us now turn to a theoretical description of second-order processes in chiral materials. We represent the second-order polarization induced in such a material as

$$P_i(\omega_\sigma) = 2\epsilon_0 \sum_{jk} \chi_{ijk}^{(2)}(\omega_\sigma = \omega_1 + \omega_2) E_j F_k, \quad (5.5.1)$$



where  $E_j$  represents a field at frequency  $\omega_1$  and  $F_k$  represents a field at frequency  $\omega_2$  (which can be a negative frequency). We now formally rewrite Eq. (5.5.1) as

$$P_i = \epsilon_0 \sum_{jk} S_{ijk} (E_j F_k + E_k F_j) + \epsilon_0 \sum_{jk} A_{ijk} (E_j F_k - E_k F_j), \quad (5.5.2)$$

where  $S_{ijk}$  and  $A_{ijk}$  denote the symmetric and antisymmetric parts of  $\chi_{ijk}^{(2)}$  and are given by

$$S_{ijk} = \frac{1}{2} (\chi_{ijk}^{(2)} + \chi_{ikj}^{(2)}), \quad (5.5.3a)$$

$$A_{ijk} = \frac{1}{2} (\chi_{ijk}^{(2)} - \chi_{ikj}^{(2)}). \quad (5.5.3b)$$

Note that  $A_{ijk}$  vanishes for second-harmonic generation or more generally whenever the Kleinman symmetry condition is valid.

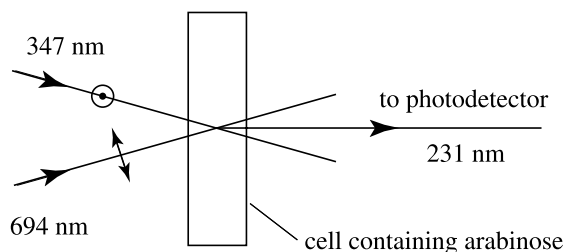


FIGURE 5.5.2: Experimental setup to observe sum-frequency generation in an isotropic, chiral medium.

The tensor properties of the quantities  $S_{ijk}$  and  $A_{ijk}$  can be deduced using methods analogous to those described in Section 1.5. For the case of an isotropic but noncentrosymmetric medium (which corresponds to point group  $\infty\infty$ ) one finds that  $S_{ijk}$  vanishes identically and that the only nonvanishing elements of  $A_{ijk}$  are

$$A_{123} = A_{231} = A_{312}. \quad (5.5.4)$$

Consequently the nonlinear polarization can be expressed as

$$\mathbf{P} = \epsilon_0 A_{123} \mathbf{E} \times \mathbf{F}. \quad (5.5.5)$$

The experimental setup used by Rentzipis et al. to study these effects is shown in Fig. 5.5.2. The two input beams are at different frequencies, as required for  $A_{123}$  to be nonzero. In addition, they are orthogonally polarized to ensure that  $\mathbf{E} \times \mathbf{F}$  is nonzero and are noncollinear to ensure that  $\mathbf{P}$  has a transverse component. Generation of a sum-frequency signal at 2314 Å was reported for both dextrorotatory and levorotatory forms of arabinose, but no signal was observed when the cell contained a racemic mixture of the two forms. The measured value of

$A_{123}$  was  $1.3 \times 10^{-18}$  m/V; for comparison note that  $d_{\parallel}$  (quartz) =  $1.61 \times 10^{-17}$  m/V. A detailed reexamination of the second-order nonlinear optical properties of this system has been presented by Belkin et al. (2001).

## 5.6 Nonlinear Optics of Liquid Crystals

Liquid crystal materials often display large nonlinear optical effects. The time scale for the development of such effects is often quite long (milliseconds or longer), but even response times this long are adequate for certain applications.

Liquid crystals are composed of large, anisotropic molecules. Above a certain transition temperature, which varies significantly among various liquid crystal materials but which might typically be  $100^{\circ}\text{C}$ , these materials exist in an isotropic phase in which they behave like ordinary liquids. Below this transition temperature, liquid crystals exist in a mesotropic phase in which the orientation of adjacent molecules becomes highly correlated, giving rise to the name *liquid crystal*. At still lower temperatures liquid crystal materials undergo another phase transition and behave as ordinary solids.

Several different types of order can occur in the mesotropic phase. Two of the most common are the nematic phase and the chiral nematic phase (which is also known as the cholesteric phase), which are illustrated in Fig. 5.6.1.

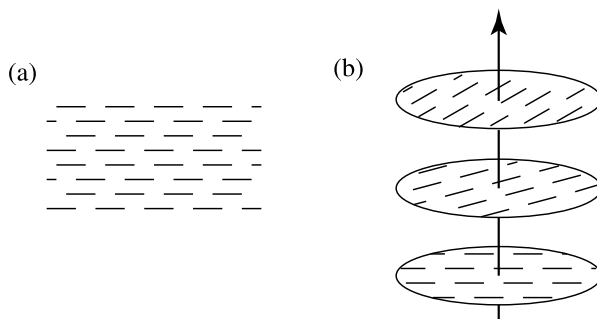


FIGURE 5.6.1: Two examples of ordered-phases (mesophases or mesotropic phases) of liquid crystals. (a) In the nematic phase, the molecules are randomly distributed in space but are aligned such that the long axis of each molecule, known as the director, points in the same direction. (b) In the chiral nematic phase, the molecules in each plane are aligned as in the nematic phase, but the director orientation rotates between successive planes.

We next present a brief summary of the development of the field of liquid-crystal nonlinear optics. As early as 1973, Wang and Shen reported an optical nonlinear response for the isotropic phase of a nematic liquid crystal. Hanson et al. (1977) reported self-focusing of light in a liquid crystal medium. Giant nonlinearities of liquid crystals in their mesotropic phase were

reported by Zeldovich et al. (1980) and by Khoo and Zhuang (1980). Janossy and Kosa (1992) showed that this response could be further increased by doping the liquid crystal with dye molecules to increase the light-matter interaction. The studies reported above were conducted using continuous wave laser radiation. Hsiung et al. (1984) reported strong nonlinear response for excitation with pulsed radiation, even for laser pulse durations significantly shorter than the response time of the liquid crystal material. Peccianti et al. (2000) reported waveguiding in liquid crystal materials assisted by the application of a static electric field. This history has been reviewed more extensively by Khoo and Shen (1985) and by Lukishova (2000). The optical properties of liquid crystals have been described more generally by Khoo (2007).

Liquid crystalline materials possess strong nonlinear optical effects in both the isotropic and mesotropic phases. In the isotropic phase, liquid crystal materials display a molecular-orientation nonlinear response of the sort described in Section 4.4, but typically with a much larger magnitude. This response is strongly temperature dependent. In one particular case, Hanson et al. (1977) find that the nonlinear coefficient  $n_2$  and the response time  $\tau$  are given by

$$n_2 = \frac{2.54 \times 10^{-15}}{n_0(T - T^*)} \frac{\text{m}^2 \text{K}}{\text{W}}, \quad T > T^*, \quad (5.6.1)$$

$$\tau = \frac{e^{2800/T(\text{K})}}{T - T^*} 7 \times 10^{-11} \text{ ns K}, \quad T > T^*, \quad (5.6.2)$$

where  $T^* = 77^\circ\text{C}$  is the liquid-crystal transition temperature. In the range of temperatures from 130 to  $80^\circ\text{C}$ ,  $n_2$  ranges from 3.2 to  $60 \times 10^{-13} \text{ cm}^2/\text{W}$  and  $\tau$  varies from 1 to 72 nsec. These  $n_2$  values are 10 to 200 times larger than those of carbon disulfide.

Liquid crystal materials possess even stronger nonlinear optical properties in the mesophase than in the isotropic phase. Once again, the mechanism is one of molecular orientation, but in this case the process involves the collective orientation of many interacting molecules. The effective nonlinear response can be as much as  $10^9$  times larger than that of carbon disulfide.

Experimental studies of nonlinear optical processes in nematic liquid crystals are often performed with the molecules anchored at the walls of the cell that contains the liquid crystal material, as shown in Fig. 5.6.2.

The analysis of such a situation proceeds by considering the angle  $\theta + \theta_0$  between the director and the propagation vector  $\mathbf{k}$  of the laser beam. Here  $\theta_0$  is this angle in the absence of the laser field and  $\theta$  is the reorientation angle induced by the laser beam. It can be shown (Khoo, 2007) that this quantity obeys the relation\*

$$K_1 \frac{d^2\theta}{dz^2} + (n_e^2 - n_o^2) \frac{|A|^2}{4\pi} \sin 2(\theta + \theta_0) = 0. \quad (5.6.3)$$

\* For definiteness we assume the geometry of Fig. 5.6.2(b), and we use gaussian units as in Khoo's treatment.

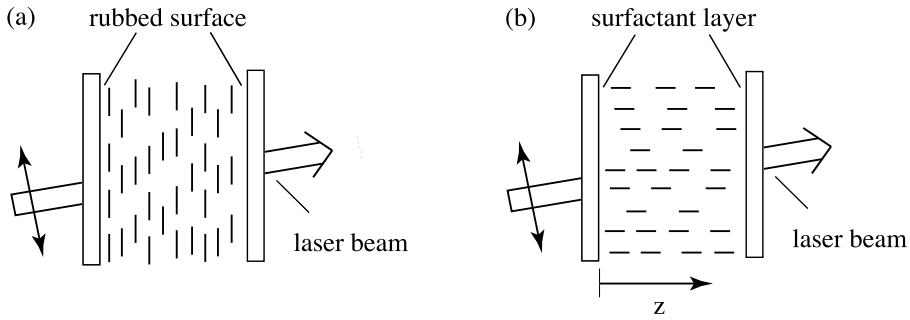


FIGURE 5.6.2: Typical cell configurations for studying optical processes in nematic liquid crystals. (a) Planar alignment: The molecules are induced to anchor at the upper and lower glass walls by rubbing these surfaces to induce small scratches into which the molecules attach. (b) Homeotropic alignment: A surfactant is applied to the cell windows to induce the molecules to align perpendicular to the plane of the window.

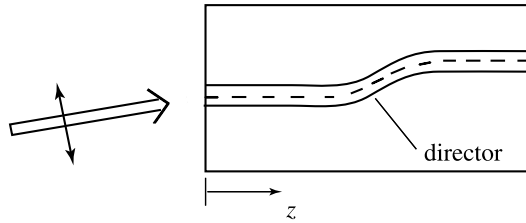


FIGURE 5.6.3: Nature of director reorientation and typical molecular alignment of a homeotropic-alignment, nematic-liquid-crystal cell in the presence of an intense laser beam.

Here  $K_1$  is an elastic constant of the liquid crystal and  $n_o$  and  $n_e$  are the ordinary and extraordinary values of the refractive index of the nematic liquid crystal in the absence of the influence of the incident laser beam. This equation is to be solved subject to the boundary conditions at the input ( $z = 0$ ) and output ( $z = d$ ) planes of the cell. Khoo and Shen (1985) shows that if this procedure is carried through one finds that the director orientation typically has the form shown in Fig. 5.6.3 and that the resulting change in refractive index, averaged over the length of the cell, can be expressed as  $\Delta n = n_2 I$  where

$$n_2 = \frac{(n_e^2 - n_o^2)^2 \sin^2(2\beta) d^2}{24K_{1c}}. \quad (5.6.4)$$

This expression can be evaluated for the conditions  $d = 100 \mu\text{m}$ ,  $n_e^2 - n_o^2 = 0.6$ ,  $K_1 = 10^{-6}(\text{dyne})$ ,  $\beta = 45^\circ$ , giving

$$n_2 = 5 \times 10^{-7} \text{ m}^2/\text{W}. \quad (5.6.5)$$

## Problems

1. *Stark shift in hydrogen.* Verify Eq. (5.1.5).
2. *Nonlinear response of the square-well potential.* Making use of the formalism of Section 5.1, calculate the linear and third-order susceptibilities of a collection of electrons confined in a one-dimensional, infinitely deep, square-well potential. Note that this calculation constitutes a simple model of the optical response of a conjugated polymer. (Hint: See Rustagi and Ducuing, 1974.)
3. *Classical calculation of the second-order response of chiral materials.* Consider an anharmonic oscillator for which the potential is of the form

$$V = \frac{1}{2}(k_a x^2 + k_b y^2 + k_c z^2) + Axyz.$$

Calculate the response of such an oscillator to an applied field of the form

$$\mathbf{E}(t) = \mathbf{E}_1 e^{-i\omega_1 t} + \mathbf{E}_2 e^{-i\omega_2 t} + \text{c.c.}$$

Then by assuming that there is a randomly oriented distribution of such oscillators, derive an expression for  $\chi^{(2)}$  of such a material. Does it possess both symmetric and antisymmetric contributions? Show that the antisymmetric contribution can be expressed as

$$\mathbf{P} = \chi_{\text{NL}} \mathbf{E}_1 \times \mathbf{E}_2,$$

$$V = \frac{1}{2}(k_a x^2 + k_b y^2 + k_c z^2) + Axyz.$$

Calculate the response of such an oscillator to an applied field of the form

$$\mathbf{E}(t) = \mathbf{E}_1 e^{-i\omega_1 t} + \mathbf{E}_2 e^{-i\omega_2 t} + \text{c.c.}$$

Then by assuming that there is a randomly oriented distribution of such oscillators, derive an expression for  $\chi^{(2)}$  of such a material. Does it possess both symmetric and antisymmetric contributions? Show that the antisymmetric contribution can be expressed as

$$\mathbf{P} = \chi_{\text{NL}} \mathbf{E}_1 \times \mathbf{E}_2.$$

## References

### Suggested Books on Molecular Nonlinear Optics for Further Reading

- Chemla, D.S., Zyss, J., 1987. *Nonlinear Optical Properties of Organic Molecules and Crystals*, vols. 1 and 2. Academic Press, New York.
- Kuzyk, M.G., Dirk, C.W. (Eds.), 1998. *Characterization Techniques and Tabulation for Organic Nonlinear Optical Materials*. Marcel Dekker, Inc..
- Prasad, P.N., Williams, D.J., 1991. *Introduction of Nonlinear Optical Effects in Molecules and Polymers*. John Wiley and Sons, New York.

**Section 5.1. Nonlinear Susceptibility . . . Time-Independent Perturbation Theory**

- Bethe, H.A., Salpeter, E.A., 1977. *Quantum Mechanics of One- and Two-Electron Atoms*. Plenum, New York.
- Dalgarno, A., 1961. In: Bates, D.R. (Ed.), *Quantum Theory*. Academic Press, New York.
- Ducuing, J., 1977. In: Bloembergen, N. (Ed.), *Proceedings of the International School of Physics "Enrico Fermi," Course LXIV*. North Holland, Amsterdam.
- Jha, S.S., Bloembergen, N., 1968. *Phys. Rev.* 171, 891.
- Sewell, G.L., 1949. *Proc. Camb. Philos. Soc.* 45, 678.
- Schiff, L.I., 1968. *Quantum Mechanics*, 3rd ed. McGraw Hill, New York. See especially Eq. (33.9).

**Section 5.2. Semiempirical Models**

- Adair, R., Chase, L.L., Payne, S.A., 1989. *Phys. Rev. B* 39, 3337.
- Boling, N.L., Glass, A.J., Owyong, A., 1978. *IEEE J. Quantum Electron.* 14, 601.
- Lenz, G., Zimmermann, J., Katsufuji, T., Lines, M.E., Hwang, H.Y., Spälter, S., Slusher, R.E., Cheong, S.-W., 2000. *Opt. Lett.* 25, 254.
- Wang, C.C., 1970. *Phys. Rev. B* 2, 2045.
- Wynne, J.J., 1969. *Phys. Rev.* 178, 1295.

**Section 5.3. Nonlinear Optics of Conjugated Polymers**

- Blau, W.J., Byrne, H.J., Cardin, D.J., Dennis, T.J., Hare, J.P., Kroto, H.W., Taylor, R., Walton, D.R.M., 1991. *Phys. Rev. Lett.* 67, 1423; see also Knize and Partanen (1992) and Kafafi et al. (1992).
- Hermann, J.P., Ducuing, J., 1974. *J. Appl. Phys.* 45, 5100.
- Kafafi, Z.H., Bartoli, F.J., Lindle, J.R., Pong, R.G.S., 1992. *Phys. Rev. Lett.* 68, 2705.
- Knize, R.J., Partanen, J.P., 1992. *Phys. Rev. Lett.* 68, 2704.
- Rustagi, K.C., Ducuing, J., 1974. *Opt. Commun.* 10, 258.

**Section 5.4. Bond Charge Model**

- Chemla, D.S., 1971. *Phys. Rev. Lett.* 26, 1441.
- Chemla, D.S., Begley, R.F., Byer, R.L., 1974. *IEEE J. Quantum Electron.* 10, 71.
- Kajzar, F., Messier, J., 1985. *Phys. Rev. A* 32, 2352.
- Levine, B.F., 1969. *Phys. Rev. Lett.* 22, 787.
- Levine, B.F., 1973. *Phys. Rev. B* 7, 2600.
- Phillips, J.C., 1967. *Phys. Rev. Lett.* 19, 415.
- Van Vechten, J.A., 1969. *Phys. Rev.* 182, 891.

**Section 5.5. Nonlinear Optics of Chiral Media**

- Belkin, M.A., Han, S.H., Wei, X., Shen, Y.R., 2001. *Phys. Rev. Lett.* 87, 113001.
- Giordmaine, J.A., 1965. *Phys. Rev.* 138, A1599.
- Jenkins, F.A., White, H.E., 1976. *Fundamentals of Optics*. McGraw-Hill, New York.
- Rentzipis, P.M., Giordmaine, J.A., Wecht, K.W., 1966. *Phys. Rev. Lett.* 16, 792.
- Verbiest, T., Van Elshocht, S., Kauranen, M., Hellemans, L., Snauwaert, J., Nuckolls, C., Katz, T.J., Persoons, A., 1998. *Science* 282, 913.

**Section 5.6. Liquid Crystal Nonlinear Optics**

- Hanson, E.G., Shen, Y.R., Wang, G.K.L., 1977. *Appl. Phys.* 14, 65.
- Hsiung, H., Shi, L.P., Shen, Y.R., 1984. *Phys. Rev. A* 30, 1453.
- Janossy, I., Kosa, T., 1992. *Opt. Lett.* 17, 1183.
- Khoo, I.C., 2007. *Liquid Crystals*, Second Edition. John Wiley, New York. See especially Chapter 8.
- Khoo, I.C., Shen, Y.R., 1985. *Opt. Eng.* 24, 244579.
- Khoo, I.C., Zhuang, S.L., 1980. *Appl. Phys. Lett.* 37, 3.

- Lukishova, S.G., 2000. J. Nonlinear Opt. Phys. Mater. 9, 365.
- Peccianti, M., De Rossi, A., Assanto, G., De Luca, A., Umeton, C., Khoo, I.C., 2000. Appl. Phys. Lett. 77, 7.
- Wang, G.K.L., Shen, Y.R., 1973. Phys. Rev. Lett. 30, 895; see also Wang and Shen ([1974](#)).
- Wang, G.K.L., Shen, Y.R., 1974. Phys. Rev. A 10, 1277.
- Zeldovich, B., Pilipetskii, N., Shkunov, A., Tabiryan, N., 1980. JETP Lett. 31, 263.